Biochimica et Biophysica Acta 1798 (2010) 872–881

Contents lists available at ScienceDirect

Biochimica et Biophysica Acta

journal homepage: www.elsevier.com/locate/bbamem

# Structure and phase behavior of *O*-stearoylethanolamine: A combined calorimetric, spectroscopic and X-ray diffraction study

Pradip K. Tarafdar, Musti J. Swamy *

*School of Chemistry, University of Hyderabad, Hyderabad - 500 046, India*

ARTICLE INFO

*Article history:*
Received 23 June 2009
Received in revised form 10 January 2010
Accepted 19 January 2010
Available online 28 January 2010

*Keywords:*
Differential scanning calorimetry
*O*-acylethanolamine
Micelle
Hydrocarbon chain tilt
Outer hyperfine splitting

ABSTRACT

Recent studies show that *O*-acylethanolamines (OAEs), structural isomers of the putative stress-fighting lipids, namely *N*-acylethanolamines (NAEs), can be derived from NAEs and are present in biological membranes under physiological conditions. In view of this, we have synthesized *O*-stearoylethanolamine (OSEA) as a representative OAE and investigated its phase behavior and crystal structure. The thermotropic phase transitions of OSEA dispersed in water and in 150 mM NaCl were characterized using calorimetric, spectroscopic, turbidimetric and X-ray diffraction studies. These studies have revealed that when dispersed in water OSEA undergoes a cooperative phase transition centered at 53.8 °C from an ordered gel phase to a micellar structure whereas in presence of 150 mM NaCl the transition temperature increases to 55.8 °C and most likely the bilayer structure is retained above the phase transition. *O*-Stearoylethanolamine crystallized in the orthorhombic space group $P2_12_12_1$ with four symmetry-related molecules in the unit cell. Single-crystal X-ray diffraction studies show that OSEA molecules adopt a linear structure with all-trans conformation in the acyl chain region. The molecules are organized in a tail-to-tail fashion, similar to the arrangement in a bilayer membrane. These studies are relevant to understanding the role of salt on the phase properties of this new class of lipids.



## 1. Introduction

Important membrane lipids such as diacyl phosphatidylethanolamine, dialkyl phosphatidylethanolamine, phosphatidylethanolamine plasmalogen and *N*-acyl phosphatidylethanolamine (NAPE) contain an ethanolamine moiety in their structure. Some other membrane lipids like phosphatidylcholine, sphingomyelin and platelet activating factor have a choline moiety — which is partly derived by the progressive methylation of ethanolamine in liver and brain [1,2]. These facts show that ethanolamine is an important building block of a variety of biologically significant lipids. Besides these membrane phospholipids, ethanolamine is also a building block of *N*-acylethanolamines (NAEs), which are fatty acid amide derivatives of ethanolamine that have been shown to stabilize the bilayer structure [3]. The content of NAEs in a wide variety of organisms increases dramatically when they are subjected to diverse types of stress, suggesting that they may be part of stress-fighting responses of the parent organisms [3,4]. In addition to their putative role in combating stress, NAEs also exhibit several other interesting biological and medicinal properties. For example, *N*-arachidonylethanolamine (anandamide) acts as an endogenous ligand of type-1 cannabinoid receptors, inhibits gap-junction conductance and reduces the fertilizing capacity of sperm [5–7], whereas *N*-palmitoylethanolamine (NPEA) acts as an agonist for the type-2 cannabinoid receptor [8]. *N*-Myristoylethanolamine (NMEA) and *N*-lauroylethanolamine are secreted into the culture medium of tobacco cells when challenged by a fungal elicitor, xylanase [9].

Besides *N*-acylation, amphiphiles can also be produced by the *O*-acylation of ethanolamine with a long acyl chain to form an ester derivative of ethanolamine, namely *O*-acylethanolamines (OAEs). Recently it has been shown that *O*-acylethanolamines are converted to *N*-acylethanolamines in a facile manner under mildly basic conditions, whereas the reverse reaction – formation of *O*-acylethanolamines from *N*-acylethanolamines – is catalyzed by acid [10]. These observations suggested the possible presence of OAEs as minor constituents in membranes as the environment of endosomes and ischemic tissues are acidic in nature [11–13]. It is likely that these minor constituents of membranes might have escaped detection for a long time due to their conversion to NAEs under conditions employed in the extraction, purification or detection (e.g., tlc using solvents containing ammonia). Interestingly, subsequent studies have led to the detection and identification of *O*-arachidonylethanolamine (virodhamine) – a structural

*Abbreviations:* OAEs, *O*-acylethanolamines; NAEs, *N*-acylethanolamines; OSEA, *O*-stearoylethanolamine; NAPE, *N*-acylphosphatidylethanolamine; NPEA, *N*-palmitoylethanolamine; NMEA, *N*-myristoylethanolamine; NSEA, *N*-stearoylethanolamine; DMAP, 4-dimethylaminopyridine; DCC, *N, N′*-dicyclohexylcarbodiimide; DSC, differential scanning calorimetry; $T_t$, transition temperature; $\Delta H_t$, enthalpy of transition; $\Delta S_t$, entropy of transition; $T_{1/2}$, the width at half maximum of the transition; ESR, electron spin resonance; $2A_{max}$, outer hyperfine splitting; LAXS, low-angle X-ray scattering; *P*, packing parameter

* Corresponding author. Tel.: +91 40 2313 4807; fax: +91 40 2301 2460.
*E-mail addresses:* mjssc@uohyd.ernet.in, mjswamy1@gmail.com (M.J. Swamy).

0005-2736/$ – see front matter © 2010 Elsevier B.V. All rights reserved.
doi:10.1016/j.bbamem.2010.01.012

isomer of anandamide – in mammalian brain, which exhibits partial agonist/antagonist activity to the type-1 cannabinoid receptor and agonist activity to the type-2 cannabinoid receptor [14]. These observations indicate that OAEs containing other fatty acyl moieties may also be present in biological membranes, with potentially interesting biological properties. In this regard it is of considerable interest to investigate the phase behavior and membrane interactions of OAEs and to identify their possible biological role. In this direction, in the present study, we have synthesized *O*-stearoylethanolamine (OSEA) and characterized its phase behavior using differential scanning calorimetry (DSC), UV–Visible spectroscopy, fluorescence spectroscopy, spin-label ESR spectroscopy and low-angle X-ray scattering (LAXS). In addition, the 3-dimensional structure of *O*-stearoylethanolamine has been investigated by single-crystal X-ray diffraction and the molecular packing and intermolecular interactions in the crystal lattice have been analyzed.

Biological membranes are surrounded by an aqueous medium that contains ions and their interactions with cell membranes are crucial for membrane fusion, phase transitions, or transport across the membrane. Several studies on model membrane systems have revealed that ions exhibit significant effects on the local and global properties of lipid bilayers [15–22]. It was also demonstrated that ionic strength can modulate the reorganization of lipids and membrane proteins in erythrocytes and affects membrane bending and shape of the erythrocytes [23,24]. In view of this, we have investigated the effect of salt on the phase behavior of *O*-stearoylethanolamine. Studies aimed at understanding the effect of salt (NaCl) concentration on the phase transition of the lipid suggest that salt most likely stabilizes the lamellar structure even at higher temperatures.

## 2. Materials and methods

### 2.1. Materials

Stearic acid, 5-doxyl stearic acid, *N, N′*-dicyclohexylcarbodiimide (DCC) and 4-dimethylaminopyridine (DMAP) were purchased from Sigma-Aldrich (USA). Ammonium chloride ($NH_4Cl$), sulfuric acid and dioxane were obtained from Merck (Germany). Ethanolamine, BOC-anhydride (di-tert-butyl dicarbonate) and all the solvents were purchased locally. Milli-Q water was used in all experiments.

### 2.2. Synthesis of O-stearoylethanolamine hydrochloride

*O*-Stearoylethanolamine hydrochloride (OSEA.HCl) was synthesized by a minor modification of the procedure reported by Markey et al. [10]. Ethanolamine was blocked using BOC-anhydride and the protected ethanolamine was condensed with stearic acid using DCC as a coupling reagent. A catalytic amount of DMAP was used in condensation. The BOC-protected ester was then deblocked with 4 M HCl in dioxane (prepared by dissolving dry HCl gas, which was produced from $NH_4Cl$ and conc. $H_2SO_4$, into dioxane) to get the hydrochloride salt of *O*-stearoylethanolamine. Purity of the product was verified by IR and $^1$H-NMR spectroscopy.

### 2.3. Differential scanning calorimetry

Differential scanning calorimetric studies were performed using a VP-DSC equipment (MicroCal LLC, Northampton, MA, USA). Accurately weighed lipid samples were dissolved in dry dichloromethane/methanol (1:1, v/v) and then the solvent was removed under a stream of dry nitrogen gas. The resulting lipid film was vacuum desiccated for 5–6 h in order to remove residual traces of the solvent. The lipid was hydrated thoroughly with Milli-Q water or with 150 mM NaCl before performing the heating scans. The pH in both cases is slightly acidic due to dissolved carbon dioxide from air. The concentration of OSEA.HCl was kept between 0.5 and 1.0 mg/ml in DSC experiments.

### 2.4. Turbidimetric studies

Samples for turbidimetric measurements were prepared by dispersing OSEA.HCl in water or 150 mM NaCl. The sample was then hydrated fully by heating to about 65–70 °C in a warm water bath, with intermittent vortexing, followed by at least five cycles of freeze thawing, using liquid nitrogen and hot water (ca. 65 °C). After the last incubation in hot water, the sample was equilibrated to room temperature and transferred to a spectrometer cuvette. Turbidimetric measurements were performed at various temperatures between 25 and 65 °C using a Cary 100 UV–Visible spectrophotometer (VARIAN) equipped with a Peltier thermostat supplied by the manufacturer. Turbidity was measured by recording the optical density (scattering) from 350 nm to 450 nm and turbidity at 400 mm was considered for further analysis.

### 2.5. ESR spectroscopy

Lipid dispersions of OSEA.HCl containing probe amounts of 5-doxyl stearic acid spin label (5-SASL) were prepared as follows. Measured volumes of OSEA.HCl stock solution (dissolved in chloroform–methanol mixture) and the spin-label stock solution were dispensed into glass sample tubes using a Hamilton syringe to give 0.5 mol% spin label in the lipid dispersion. The solvent was evaporated by a gentle stream of dry nitrogen gas and the residual traces of the solvent were removed by vacuum desiccation for a minimum of 3 h. The samples were then hydrated with water or 150 mM NaCl and kept in the dark at room temperature to reach equilibrium. Then the samples were centrifuged, and the pellets were transferred to glass capillaries. ESR spectra were recorded on a JEOL JES-FA 200 ESR spectrometer. Samples in 1 mm ID glass capillaries were placed in a standard quartz ESR tube containing light silicone oil for thermal stability. Temperature was measured with a fine-wire thermocouple positioned near the ESR tube.

### 2.6. Fluorescence spectroscopy

Fluorescence measurements were made on a SPEX FLUOROMAX-4 fluorescence spectrometer equipped with a temperature controller supplied by the manufacturer. Samples for fluorescence experiments were prepared essentially in the same manner as described above for ESR experiments, except that instead of spin probe pyrene was used. The lipid was then hydrated with water or with 150 mM NaCl and the optical density of the sample at 335 nm was kept below 0.1. The lipid: pyrene ratio was kept as 400:1 and the final pyrene concentration was kept in the μM range. Samples were excited at 335 nm and emission spectra were recorded between 350 and 550 nm. Each spectrum was blank subtracted and corrected for lamp intensity variation during measurement. The excitation and emission slit widths were set at 1.5 nm. Pyrene exhibits five bands in the emission spectrum and the ratio of intensities of the first and third peaks ($I_1/I_3$) was used in the analysis of the fluorescence data.

### 2.7. Crystallization, X-ray diffraction and structure solution

Thin needle type, colorless crystals of *O*-stearoylethanolamine hydrochloride were grown at room temperature from dichloromethane, containing a trace of methanol. A crystal of $0.42\times0.32\times0.08$ mm size was used for data collection. X-ray diffraction measurements were carried out at room temperature (ca. 25 °C) with a Bruker SMART APEX CCD area detector system using a graphite monochromator and Mo-Kα ($\lambda = 0.71073$ Å) radiation obtained from a fine-focus sealed tube.

Data reduction was done using Bruker SAINTPLUS program. Structure solution was carried out in the orthorhombic space group. Absorption correction was applied using SADABS program. The structure was solved successfully by direct methods in the space group

$P2_12_12_1$ and refinement was done by full matrix least-squares procedure using the SHELXL-97 program [25]. The refinement converged into a final $R_1 = 0.167$, w$R_2 = 0.432$ and goodness of fit = 1.36.

### 2.8. Crystal parameters of O-stearoylethanolamine hydrochloride

Molecular formula: $C_{20}H_{42}ClNO_2$. Molecular formula weight: 364.0; Crystals were needle-shaped and colorless. Crystal system, Orthorhombic; Space group, Sg = $P2_12_12_1$; Ambient temperature, $T = 298(2)$ K; Radiation wavelength ($\lambda$) = 0.71073 Å; Radiation type, Mo-K$\alpha$; Radiation source, Fine-focus sealed tube; Radiation monochromator, graphite; Number of reflections collected, 20538; Unique reflections, 3963; Reflection with $I > 2\sigma(I)$, 2289; Number of parameters, 219.

Unit cell dimensions (with standard deviation in parentheses): $a = 5.382(5)$, $b = 5.410(5)$, $c = 79.98(7)$ Å; Volume of the cell, $V = 2328(3)$ Å$^3$; Density, $D_{Calc} = 1.038$ g cc$^{-1}$; Number of molecules in the unit cell, $Z = 4$; Angle of tilt of *O*-acyl chains, $\theta = 44.4°$; $F_{(000)} = 808$; Absorption Coefficient, $\mu = 0.175$ mm$^{-1}$; $T = 298(2)$ K.

### 2.9. Low-angle X-ray scattering

LAXS measurements with OSEA.HCl dispersed in water and in 150 mM NaCl were recorded using a Hecus S3-Micro System (Graz, Austria) equipped with a one-dimensional position sensitive detector. Samples were filled in sealed 1 mm diameter quartz capillaries and kept in good thermal contact with a programmable Peltier unit, which allows temperature control in the range of 0 °C to 65 °C. Samples were equilibrated for 10 min at each temperature prior to measurement. The exposure time was set to 1000 s and the diffraction patterns were calibrated using silver behenate.

## 3. Results

### 3.1. Differential scanning calorimetry

*O*-Stearoylethanolamine (OSEA) has a basic moiety (–$NH_2$ group), which can exist in the protonated or free state depending upon the environment. Since *O*-acylethanolamines are not stable at basic pH [10] and in view of the acidic pH of endosomes and ischemic tissues [11–13], we have synthesized *O*-stearoylethanolamine as the hydrochloride and characterized its phase transition. The hydrated *O*-stearoylethanolamine hydrochloride (OSEA.HCl) yielded turbid suspensions at room temperature, which became optically clear at higher temperature, suggesting that the amphiphile undergoes a phase transition from a phase of high turbidity (possibly lamellar gel phase) to a phase where aggregates are small (such as micelles), which do not scatter visible light.

In order to characterize the thermotropic transitions we have carried out differential scanning calorimetric studies on OSEA.HCl in excess water. The DSC thermogram gave a single transition centered at 53.8 °C (Fig. 1). Thermodynamic parameters such as transition temperature ($T_t$), enthalpy of transition ($\Delta H_t$), entropy of transition ($\Delta S_t$) and the width at half maximum of the transition ($T_{1/2}$) obtained from DSC studies are listed in Table 1. In order to understand the effect of ionic strength on the phase transition the calorimetric studies were performed at various concentrations of NaCl. A representative heating thermogram recorded in 150 mM NaCl is also shown in Fig. 1 and the thermodynamic parameters obtained are listed in Table 1. These data show that increasing the salt concentration results in an increase in the phase transition temperature ($T_t$), whereas the corresponding width at half maximum of the transition ($T_{1/2}$) decreases. Since the transition temperature does not change above 150 mM NaCl, further studies regarding the salt concentration dependence on the phase behavior and phase transition have been carried out at the same concentration of NaCl. It is noteworthy that this ionic strength is physiologically relevant. The increase in $T_t$ in presence of salt suggests that salt may stabilize the gel phase, which is most likely of the lamellar structure (see below) whereas the decrease in $T_{1/2}$ with increase in the salt concentration shows that the phase transition becomes sharper. Saturated diacylphosphatidylcholines are known to exhibit sharp, thermotropic lamellar gel–liquid crystalline phase transitions with increase in temperature. The widths at half height ($T_{1/2}$) of these sharp transitions range between 0.10 and 0.32° for lamellar gel–liquid crystalline phase transition in phosphatidylcholines ($n = 13$–20) [26,27]. The $T_{1/2}$ of 0.57 °C observed for the phase transition of OSEA.HCl in water (Table 1) is higher than the value obtained for the gel–liquid crystalline phase transition in hydrated distearoylphosphatidylcholine (DSPC) ($T_t = 55.3$ °C, $T_{1/2} = 0.24$ °C) [27]. The comparison with DSPC is appropriate in view of the fact that both DSPC and OSEA.HCl have identical (stearoyl) acyl chains in the hydrophobic region. The higher $T_{1/2}$ observed here for OSEA.HCl in water suggests that the phase transition is broader and hence may not correspond to a lamellar gel-to-liquid crystalline transition, which in phosphatidylcholines is a rather sharp transition. Additionally, as the solution becomes transparent at high temperature, it is likely that OSEA.HCl exists as micelles above the phase transition i. e., the

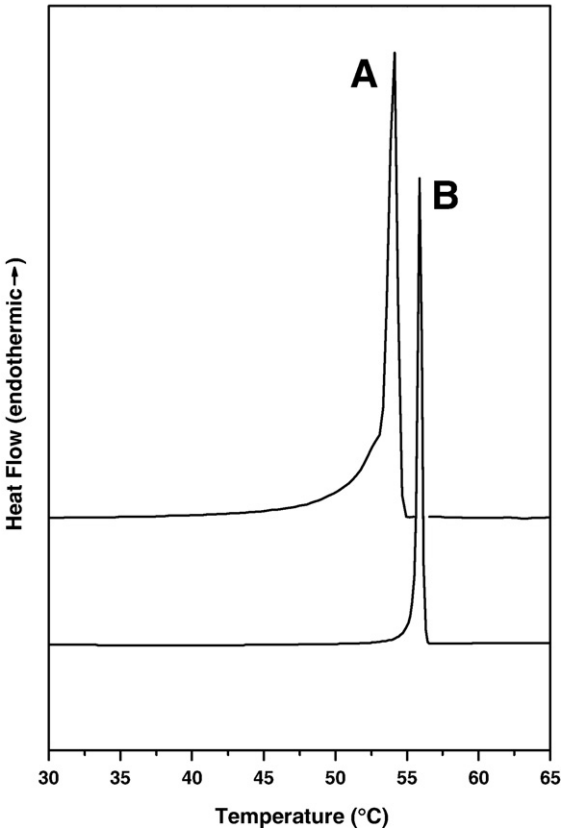


**Fig. 1.** DSC heating thermograms of *O*-stearoylethanolamine hydrochloride dispersed in (A) water and (B) 150 mM NaCl.

**Table 1**
Thermodynamic parameters obtained from DSC studies on OSEA.HCl. Samples were dispersed in distilled water containing the indicated concentration of sodium chloride.

| NaCl (mM) | $T_t$ (°C) | $T_{1/2}$ (°) (in Celsius scale) | $\Delta H_t$ (kcal mol$^{-1}$) | $\Delta S_t$ (cal mol$^{-1}$ K$^{-1}$) |
|---|---|---|---|---|
| 0 | 53.8 ± 0.37 | 0.57 ± 0.19 | 5.27 ± 0.73 | 16.12 |
| 25 | 55.24 ± 0.16 | 0.43 ± 0.04 | 6.35 ± 0.12 | 19.32 |
| 50 | 55.58 ± 0.24 | 0.34 ± 0.02 | 4.92 ± 0.07 | 14.97 |
| 150 | 55.81 ± 0.24 | 0.36 ± 0.06 | 5.45 ± 0.80 | 16.57 |
| 250 | 55.84 ± 0.10 | 0.30 ± 0.04 | 5.77 ± 1.24 | 17.54 |

transition taking place in water may corresponds to a lamellar gel to micellar phase transition. In the presence of 150 mM NaCl the $T_{1/2}$ and the $T_t$ values obtained from DSC studies for OSEA.HCl ($T_t$ = 55.8 °C, $T_{1/2}$ = 0.36 °C) are comparable to those corresponding to the gel–liquid crystalline phase transition of DSPC ($T_t$ = 55.3 °C, $T_{1/2}$ = 0.24 °C). Since the $T_t$ increases and $T_{1/2}$ decreases and the sample remains turbid above phase transition, it is clear that salt has a significant effect on the phase transition and the phase structure above the transition. In order to investigate this in more detail, and to characterize the high temperature phases, turbidimetric and spectroscopic studies were performed.

### 3.2. Turbidimetric studies on OSEA.HCl

To investigate the salient features of the phase transition of OSEA.HCl, turbidimetric studies have been performed, monitoring the turbidity at 400 nm as a function of temperature using a spectrophotometer. Fig. 2 depicts the change in turbidity of OSEA.HCl in water and in 150 mM NaCl. In both environments the turbidity at low temperature was relatively high, which decreases with increase in temperature. Near the phase transition temperature the turbidity exhibits a sharp decrease upon increase of temperature and thereafter remains at a constant level. The midpoint of the steeply declining region was taken as the phase transition temperature ($T_t$). The $T_t$ values obtained from the turbidimetric studies were 51.5 and 54.5 °C, respectively, for measurements performed in water and in 150 mM NaCl. These values are in good agreement with the values obtained from the DSC studies, presented above. From Fig. 2 it can be clearly seen that above phase transition temperature turbidity of the sample in water is significantly lower than that of the sample prepared in 150 mM NaCl. The difference in turbidity is not due to difference in the lipid concentration since identical concentrations of OSEA.HCl were used in these two experiments. Visual inspection indicated that above phase transition the sample prepared in water is clear to the naked eye (Fig. 3A), suggesting that the aggregates are relatively small, and most likely correspond to micelles. Above phase transition temperature the sample in 150 mM NaCl exhibits a bluish turbidity, suggesting the presence of larger aggregates (Fig. 3B), which may correspond to liquid crystalline phase.

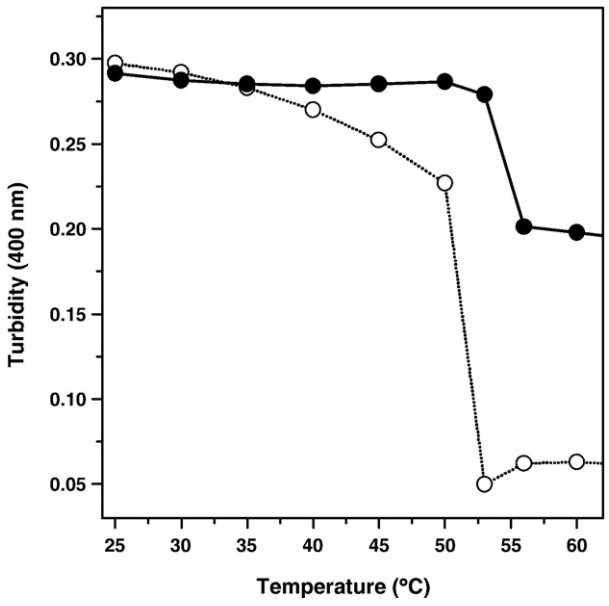


**Fig. 2.** Turbidimetric study of the thermotropic phase transition of OSEA.HCl dispersed in water (○) and in 150 mM NaCl (●). Turbidity was recorded in a spectrophotometer. Lipid concentration was 1 mg/ml for both samples.

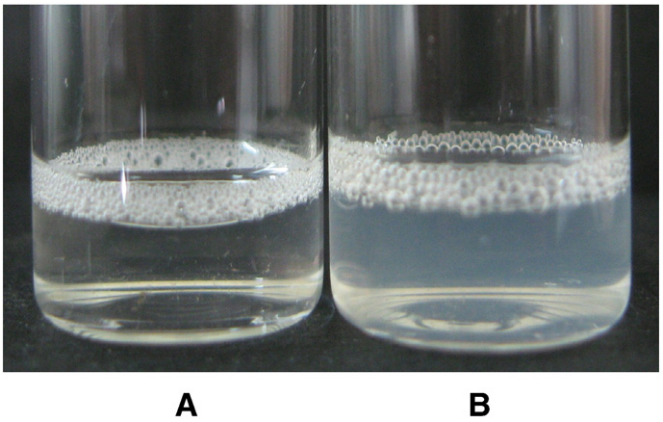


**Fig. 3.** Snapshot of OSEA.HCl above phase transition. (A) Dispersed in water and (B) dispersed in 150 mM NaCl.

### 3.3. Spin-label ESR spectroscopy

ESR spectra of 5-SASL in OSEA.HCl in water and in 150 mM NaCl recorded at different temperatures are shown in Fig. 4A and B. At 25 °C the spectra recorded in water and in 150 mM NaCl exhibit a pattern that is typical of fatty acid spin probes embedded in phospholipid bilayers [21,28,29]. The outer hyperfine splitting ($2A_{max}$), which gives a measure of anisotropic motion of the probe, is 59.2 G and 56.8 G, respectively, in water and in 150 mM NaCl. The value of $2A_{max}$ at room temperature is close to the value exhibited by fatty acid spin labels bearing the nitroxide probe on the 5th C-atom incorporated in the lamellar gel phase of lipids, suggesting that OSEA.HCl may adopt a lamellar gel phase in both the environments at room temperature [29–31]. As the temperature increases the $2A_{max}$ decreases in both environments, consistent with the environment of the probe becoming less rigid at higher temperatures (Fig. 4C). In water, the spectra become more isotropic after the phase transition. Qualitatively similar spectra have been obtained with octadecyltrimethylammonium bromide micelles and other micelles using 5-SASL as a spin probe [32]. This suggests that in water OSEA.HCl may form some kind of micelles above the phase transition temperature. This observation is consistent with the results of the above turbidimetric studies, which could be interpreted in terms of the formation of micelles by OSEA.HCl above the phase transition. In 150 mM NaCl above phase transition temperature (55 °C) the $2A_{max}$ was found to be ca. 42.6 G, which is in the range expected for the liquid crystalline phase of a bilayer membrane [30,31,33]. Also, the spectra recorded above phase transition temperature display features that are characteristic of a fluid liquid crystalline phase with partially motionally averaged, axial hyperfine anisotropy [29]. These results are in agreement with OSEA.HCl undergoing a lamellar gel phase to a fluid liquid crystalline phase transition in the presence of salt, instead of transforming to micellar phase as concluded above for the sample hydrated with water.

### 3.4. Fluorescence spectroscopy

The relative intensities of vibronic bands in pyrene monomer fluorescence exhibit good correlation with polarity of the environment in which the probe is located [34]. Higher values of $I_1/I_3$ peak ratio indicate higher polarity of the probe environment. In phospholipids, simple monitoring of the $I_1/I_3$ peak ratio allows determination of the gel-to-liquid crystalline phase transition temperature [35]. The $I_1/I_3$ peak ratio of pyrene in OSEA.HCl decreases with increase in temperature (Fig. 5), suggesting that below the phase transition temperature (gel phase) pyrene is presumably located near the head

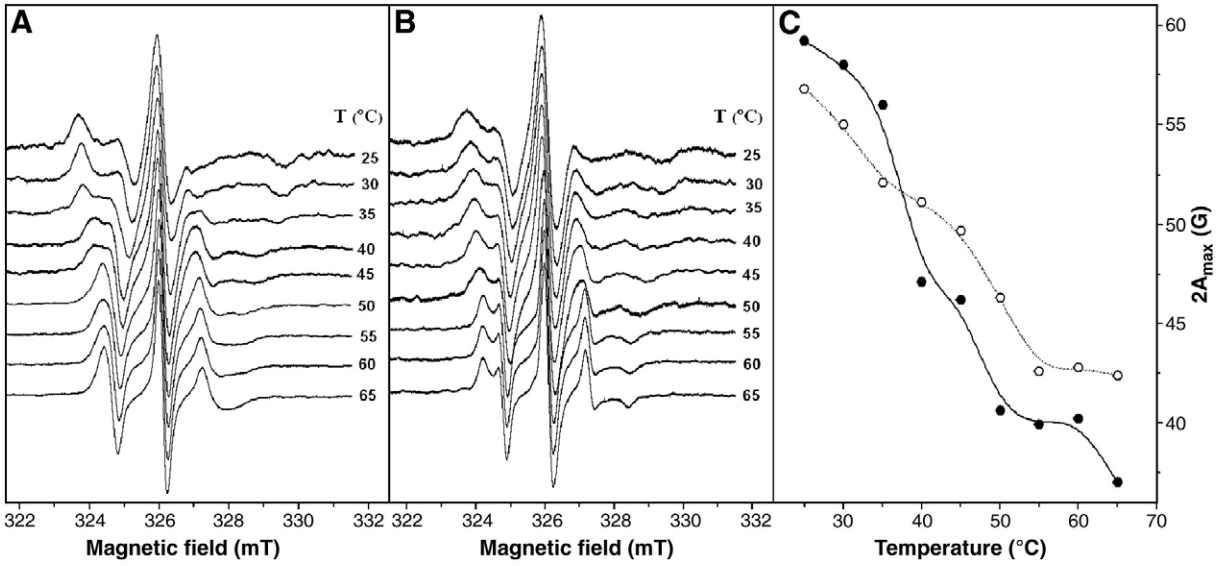


**Fig. 4.** A) ESR spectra of 5-SASL in OSEA.HCl dispersed in water. B) ESR spectra of 5-SASL in OSEA.HCl dispersed in 150 mM NaCl. C) Temperature dependence of $2A_{max}$ (G) in water (●) and in 150 mM NaCl (○). In A and B the temperature at which each spectrum was recorded is indicated.

group (polar) region and above the phase transition temperature, pyrene moves deeper into the hydrophobic region of the lipid aggregate. At room temperature (i.e., in the gel phase) $I_1/I_3$ peak ratio of OSEA.HCl in water and in 150 mM NaCl has values of 1.39 and 1.59, respectively. The higher value of peak ratio in 150 mM NaCl may be due to the fact that the environment becomes more polar at high ionic strength. It may also be possible that salt induces tighter packing of acyl chains and thus pyrene penetration to bilayer is further prohibited, resulting in its immobilization near the head group region.

### 3.5. Single-crystal X-ray diffraction studies

#### 3.5.1. Description of the structure

Since spectroscopic studies have shown that preferred conformations of acyl chains observed in solid state by X-ray analyses are predominant also in the gel phase of lipids [36], determination of the 3-dimentional structure of lipids in the solid state by single-crystal X-ray diffraction and analyzing the intermolecular interactions will be of immense value in understanding the structure and organization in the hydrated state. Therefore, we have determined the 3-dimensional structure of OSEA.HCl and its molecular packing and intermolecular interaction have been analyzed. The molecular structure of *O*-stearoylethanolamine hydrochloride is shown in the ORTEP plot given in Fig. 6. The bond distances, bond angles and torsion angles involving all the non-hydrogen atoms are given in Table 2. It is clearly seen from Fig. 6 that the hydrocarbon portion (C4–C20) of the acyl chains is in all-*trans* conformation. The torsion angles observed for the acyl chain region are all close to 180° (Table 2). The all-*trans* conformation of the acyl chain region, where all the torsion angles are close to 180°, gives the molecule a linear geometry. In NAEs such as *N*-myristoylethanolamine, *N*-palmitoylethanolamine and *N*-stearoylethanolamine, existence of a single gauche conformation in the acyl chain region results in a bending of the *N*-acyl chain, giving an 'L' shape to the molecules in the crystalline state [37–39]. Thus, there is a significant difference in the acyl chain conformation between NSEA and the *O*-stearoyl isomer of NSEA, due to which the molecular geometry changes from a bent structure in the NAEs to a linear structure in OSEA.HCl.

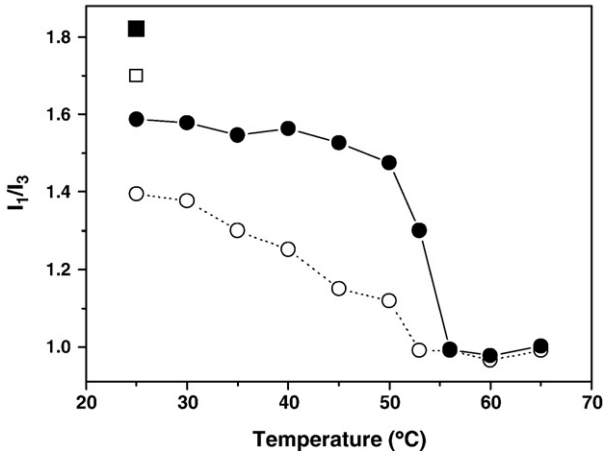


**Fig. 5.** Temperature dependence of polarity ratio ($I_1/I_3$) of pyrene in OSEA.HCl dispersed in water (○) and in 150 mM NaCl (●). Values of $I_1/I_3$ of pyrene alone in water (□) and in 150 mM NaCl (■) are also shown.

#### 3.5.2. Molecular packing

Packing diagrams of OSEA.HCl along the *a*-axis and the *b*-axis are given in Fig. 7A and B, respectively. The OSEA.HCl molecules are packed in a head-to-head (and tail-to-tail) manner in stacked bilayers. The hydrocarbon chains in the bilayer make an angle of 110° with each other, resulting in a 'V' shaped arrangement of the two interacting chains in the bilayer (Fig. 7A), whereas in NAEs the angle between adjacent hydrocarbon chains in the bilayer is nearly 180° (i.e., collinear arrangement of the chains) [37–39]. The methyl ends of the stacked bilayers are in van der Waals contacts, with the closest methyl–methyl contact distance (C20–C20) between the opposing layers and within the same layer being 3.95 Å and 5.41 Å, respectively. The bilayer thickness (N1–N1 distance) of OSEA.HCl is 37.1 Å and the all-*trans* acyl chains are tilted by 44.4° with respect to bilayer normal, which is considerably higher than the tilt angles of 34.5–37° observed in the crystal structures of NAEs [38,39]. The relatively high tilt angle in OSEA HCl as compared to NAEs may be due to the presence of bulky $Cl^-$ anion. This suggests that acyl chain packing can be modulated by the size of counter anions.

The different lateral packing modes, adopted by hydrocarbon chains in lipid crystals are generally described by subcells that specify the relations between equivalent positions within the chain and its neighbors. Examination of the hydrocarbon chain packing in the *O*-acyl chains of OSEA.HCl revealed that the hydrocarbon chains pack according to the

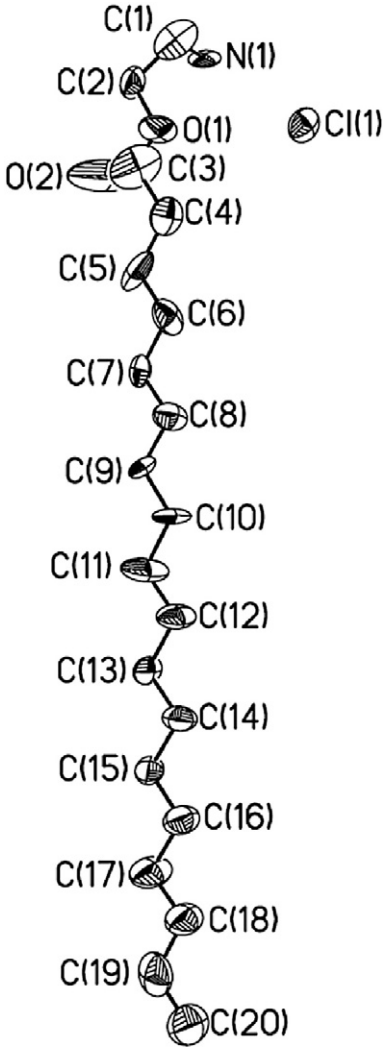


**Fig. 6.** An ORTEP plot showing the molecular structure of *O*-stearoylethanolamine hydrochloride.

triclinic subcell ($T_{//}$) [40,41]. The unit cell dimensions of these subcells are $a = 5.41$ Å, $b = 4.94$ Å and $c = 2.54$ Å.

### 3.5.3. Hydrogen bonding and intermolecular interactions

To understand the intermolecular interactions in OSEA.HCl, the molecular packing in the crystal lattice was examined from various angles. The observed hydrogen bonding pattern in the crystal lattice is shown in Fig. 8. Fig. 8A shows that each chloride ion is hydrogen bonded to three N–H hydrogens and that the chloride ion acts as a bridge between the head groups coming from opposite layers and adjacent layers. This results in the formation of three distinct hydrogen bonds by each chloride ion, with the hydrogen bond distance (H···Cl) and angle of the three types of N–H···Cl interactions being 2.29 Å, 2.30 Å, 2.28 Å and 168.0°, 158.1°, 172.4°, respectively. The three types of N–H···Cl interactions give rise to a hydrogen bonding motif in the head group region, which is topologically similar to the arrangement observed in super black phosphorous [42] (Fig. 8B). Besides the N–H···Cl interactions, weak C–H···O interaction between the carbonyl oxygen (O2) and an H-atom on C4 (carbon atom α- to the ester carbonyl) of an adjacent molecule in the same layer was observed (Fig. 8A). The C–H···O hydrogen bond connects adjacent OSEA.HCl molecules in the same plane and all the C–H···O H-bonds have the same H···O distance of 2.47 Å. The C–H···O hydrogen bond is non-linear with the angle between the covalent bond and hydrogen bond being 138.5°.

### 3.6. Low-angle X-ray scattering studies

Fig. 9 gives LAXS profiles of OSEA dispersed in water and in 150 mM NaCl. In both cases only a single sharp reflection was observed below the phase transition temperature, over the scattering range studied. Although the single reflection does not unambiguously confirm that the structure is lamellar, it is likely that the phase is lamellar. Supporting evidence for this comes from, although indirect, single-crystal X-ray diffraction studies of OSEA, which adopts a lamellar structure in the crystalline phase, with a bilayer thickness (N1–N1 distance) of 37.1 Å. The LAXS data presented in Fig. 9 indicate that at 25 °C OSEA.HCl dispersed in water and in 150 mM NaCl has repeat spacings of 39.6 and 40.0 Å, respectively, which are higher than the value obtained from the crystal structure determination. However, it should be noted that the spacings measured in the hydrated samples correspond to the combined thickness of the lipid bilayer and the

**Table 2**
Selected bond distances, bond angles and torsion angles for OSEA.HCl.

| Bond distances (Å) | | Bond angles (degree) | | Torsion angles (degree) | |
|---|---|---|---|---|---|
| O(1) – C(2) | 1.449(15) | C(2) – O(1) – C(3) | 119.0(11) | C(3) O(1) C(2) C(1) | −168.9(14) |
| O(1) - C(3) | 1.11(2) | N(1) – C(1) – C(2) | 103.7(9) | C(2) O(1) C(3) O(2) | 29(3) |
| O(2) – C(3) | 1.15(2) | O(1) – C(2) – C(1) | 107.2(8) | C(2) O(1) C(3) C(4) | 170.0(12) |
| N(1) – C(1) | 1.447(12) | O(1) – C(3) – O(2) | 121(2) | N(1) C(1) C(2) O(1) | 73.7(11) |
| C(1) – C(2) | 1.563(14) | O(1) – C(3) – C(4) | 117.0(15) | O(1) C(3) C(4) C(5) | −176.9(14) |
| C(3) – C(4) | 1.51(2) | O(2) – C(3) – C(4) | 111.0(17) | O(2) C(3) C(4) C(5) | −33(2) |
| C(4) – C(5) | 1.574(17) | C(3) – C(4) – C(5) | 119.2(11) | C(3) C(4) C(5) C(6) | −170.0(12) |
| C(5) – C(6) | 1.488(16) | C(4) – C(5) – C(6) | 115.9(9) | C(4) C(5) C(6) C(7) | −173.5(9) |
| C(6) – C(7) | 1.567(15) | C(5) – C(6) – C(7) | 113.9(9) | C(5) C(6) C(7) C(8) | −177.4(10) |
| C(7) – C(8) | 1.488(14) | C(6) – C(7) – C(8) | 112.4(8) | C(6) C(7) C(8) C(9) | 169.4(9) |
| C(8) – C(9) | 1.472(14) | C(7) – C(8) – C(9) | 115.5(8) | C(7) C(8) C(9) C(10) | 171.4(9) |
| C(9) – C(10) | 1.474(14) | C(8) – C(9) – C(10) | 118.9(8) | C(8) C(9) C(10) C(11) | −179.2(9) |
| C(10) – C(11) | 1.526(15) | C(9) – C(10) – C(11) | 121.3(9) | C(9) C(10) C(11) C(12) | −179.0(9) |
| C(11) – C(12) | 1.445(15) | C(10) – C(11) – C(12) | 118.0(9) | C(10) C(11) C(12) C(13) | −178.2(9) |
| C(12) – C(13) | 1.557(15) | C(11) – C(12) – C(13) | 116.0(9) | C(11) C(12) C(13) C(14) | 179.1(10) |
| C(13) – C(14) | 1.474(15) | C(12) – C(13) – C(14) | 116.2(8) | C(12) C(13) C(14) C(15) | −178.8(9) |
| C(14) – C(15) | 1.545(17) | C(13) – C(14) – C(15) | 113.7(9) | C(13) C(14) C(15) C(16) | −175.7(10) |
| C(15) – C(16) | 1.513(15) | C(14) – C(15) – C(16) | 113.2(9) | C(14) C(15) C(16) C(17) | 176.3(10) |
| C(16) – C(17) | 1.536(17) | C(15) – C(16) – C(17) | 114.0(9) | C(15) C(16) C(17) C(18) | 177.1(10) |
| C(17) – C(18) | 1.458(17) | C(16) – C(17) – C(18) | 111.8(10) | C(16) C(17) C(18) C(19) | −175.3(10) |
| C(18) – C(19) | 1.601(19) | C(17) – C(18) – C(19) | 114.0(10) | C(17) C(18) C(19) C(20) | −174.2(12) |
| C(19) – C(20) | 1.51(2) | C(18) – C(19) – C(20) | 114.2(12) | | |

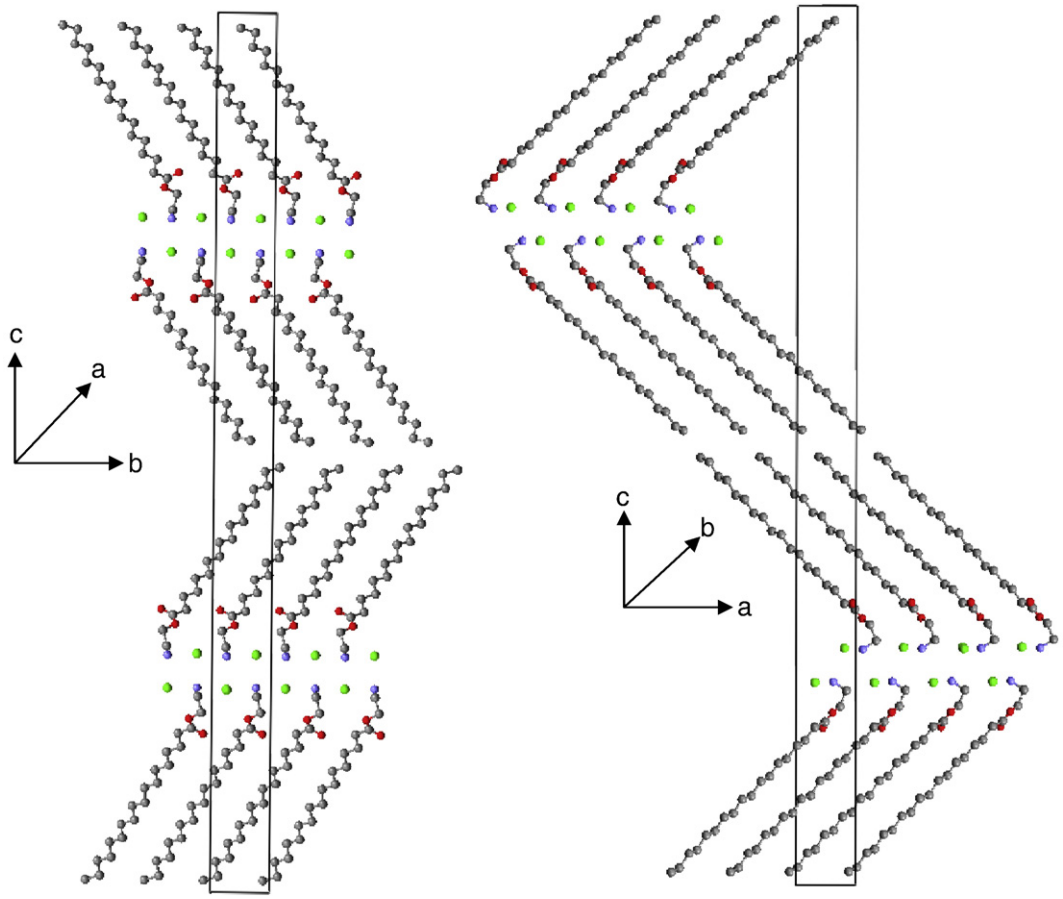


**Fig. 7.** Packing diagrams of OSEA.HCl. (A) A view along the *a*-axis. (B) A view along the *b*-axis. Dimensions of the unit cell are: $a = 5.382(5)$, $b = 5.410(5)$, $c = 79.98(7)$ Å. Color legend: red, oxygen; grey, carbon; blue, nitrogen; green, chlorine. (For interpretation of the references to color in this figure legend, the reader is referred to the web version of this article.)

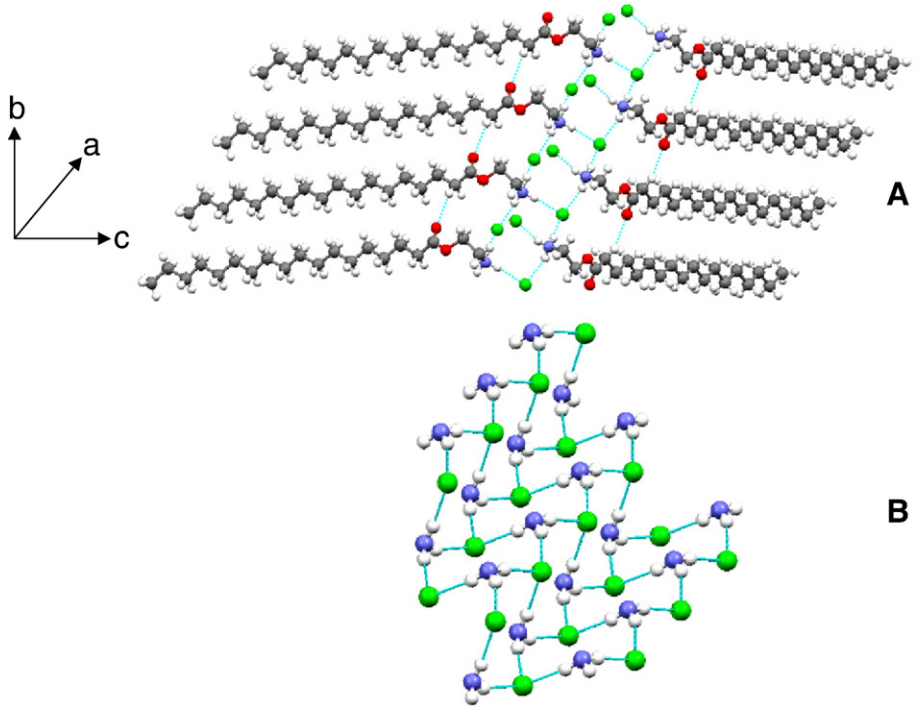


**Fig. 8.** Hydrogen bonding pattern in the crystal lattice of OSEA.HCl. (A) A close-up view displaying N–H···O type and C–H···O type hydrogen bonding. (B) Hydrogen bonded motif involving N–H···Cl interactions is topologically similar to super black phosphorous. Color legend: red, oxygen; grey, carbon; blue, nitrogen; white, hydrogen; green, chlorine.

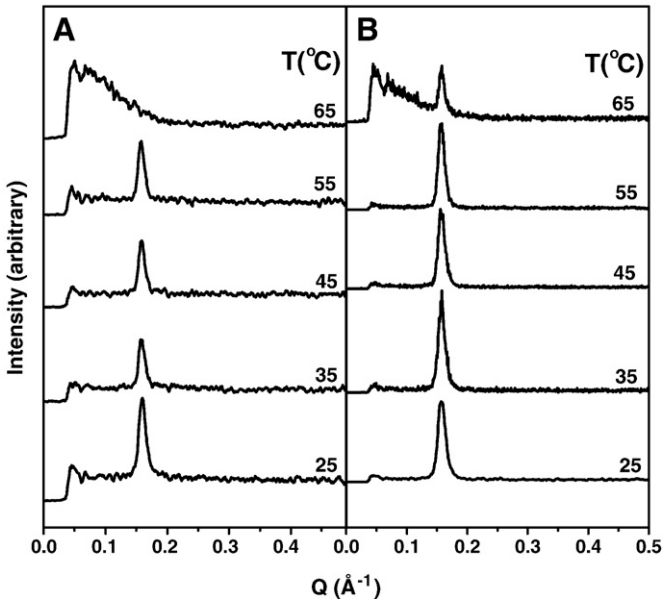


**Fig. 9.** Low-angle X-ray scattering patterns of OSEA.HCl dispersed in A) water, B) in 150 mM NaCl. The temperature at which the data were collected is indicated.

water layer between adjacent bilayers. If the tilt angle of the acyl chains with respect to the bilayer normal is comparable to that observed in the crystal structure (44.4°), then the additional spacing of ca. 3 Å would correspond to the thickness of the water layer between adjacent bilayers. If the tilt angle is less than 44.4°, then the water layer thickness would be correspondingly less, whereas for larger tilt angles the water layer thickness will be more than 3 Å. Further wide-angle X-ray scattering studies are required to investigate this in more detail.

It is pertinent to mention here that hydrated *N*-palmitoylethanolamine also exhibits a single sharp reflection in LAXS studies, which was interpreted as arising from the lamellar phase [43]. Similarly, LAXS studies on various surfactant systems also yielded single sharp reflections, which were interpreted as due to the lamellar structure [44,45]. It is possible that the higher order peaks are absent due to low electron density of head group of OAEs and NAEs as compared to phospholipids where electron-rich phosphorous is present. It is also possible that the second order reflection could be missing due to the phasing problem [cf. 46].

The peak position in both the cases (samples prepared in water and in 150 mM NaCl) does not change significantly with temperature below $T_t$. Above $T_t$ (65 °C), the sample prepared in water exhibits a broad scatter, which most likely indicates a micellar structure. For the sample prepared in 150 mM NaCl above phase transition temperature (65 °C), the sharp peak is still seen although the intensity decreases significantly and some underlying broad scatter is seen (Fig. 9).

## 4. Discussion

Research work done since the early 1960 s has shown that long-chain *N*-acylethanolamines are present as minor components in a variety of organisms and their content increases dramatically under different types of stress [3,4]. Additionally, it has been shown that NAEs can be transformed to *O*-acylethanolamines in acidic medium whereas the reverse transformation i.e., conversion of OAEs to NAEs takes place at basic pH [10]. This suggested that OAEs are also likely to be present in biomembranes, especially under stress conditions when the content of NAEs increases quite significantly. Indeed this proved to be the case when *O*-arachidonylethanolamine was found to be present in brain tissues and it was shown that it can bind to the cannabinoid receptors, type-1 and type-2 [14]. In view of this, it is of great interest to investigate the structure, phase properties and membrane interactions of *O*-acylethanolamines and to compare them with those of *N*-acylethanolamines, which are structural isomers of OAEs. While several studies have been carried out on the phase behavior of aqueous dispersions of NAEs and their interaction with other membrane lipids with a view to correlate the diverse biological activities exhibited by them [47–53], there have been no reports of similar studies on OAEs. In view of this lacuna, we have synthesized *O*-stearoylethanolamine hydrochloride and investigated its phase behavior and aggregation properties in aqueous dispersions. The results obtained are discussed here.

The self-aggregation of lipids and surfactants is an interesting phenomenon. Above a critical concentration these amphiphiles form aggregated structures and the aggregate morphology depends on the well-known packing parameter ($P$) as described by Israelachvili [54]:

$$P = v / l_c a_o$$

where $v$ and $l_c$ are the volume and chain length of the hydrophobic portion, respectively, and $a_o$ is the optimal surface area occupied by the molecule at the hydrocarbon interface. For charged amphiphiles $a_o$ is influenced considerably by the electrostatic repulsion between adjacent head groups in the aggregates and reducing the electrostatic repulsion can increase the value of $P$. Most short, single-chain surfactants have a $P$ of less than one-third and consequently form spherical micelles. For membrane lipids and double-tailed surfactants, the volume of the hydrophobic region ($v$) is increased as compared to single-chain lipids, resulting in a $P$ value in the one-half to one range, and they will adopt a bilayer or vesicular phase.

The results obtained from calorimetric and spectroscopic studies indicate that the structure of OSEA.HCl formed in aqueous dispersion depends on the ionic strength of the medium. In the absence of salt, due to electrostatic repulsion between the lipid head groups of adjacent layers OSEA.HCl takes up large amounts of water. The hydration of head group generally makes it large compared to the tail which may induce the formation of tilted lamellar gel phase at room temperature, which undergoes a phase transition with increase in temperature to yield most likely a micellar phase which was found to be optically clear in turbidimetric measurements (Fig. 2). In presence of salt the phase transition temperature increases with increase in the salt concentration and also the transition becomes sharp, which was evidenced by a decrease in the $T_{1/2}$ value (Table 1). This may be due to better packing of the hydrocarbon chains as the electrostatic repulsion will be screened in the presence of salt. The corresponding $T_t$ and $T_{1/2}$ found in OSEA.HCl are 55.8 and 0.36 °C, which are close to the values obtained for the gel–liquid crystalline phase transition temperature of distearoylphosphatidylcholine [27]. The corresponding enthalpy of transition was 5.45 kcal $mol^{-1}$, which is nearly half of the enthalpy of transition determined for the lamellar gel to liquid crystalline phase transition of DSPC [27]. This could be attributed to the fact that DSPC contains two fatty acyl chains, whereas OSEA.HCl is a single-chain lipid. Although DSC studies cannot give information on the structure of the phase, the thermodynamic parameters obtained here when taken together with the results from LAXS measurements and other studies (discussed below) are consistent with the interpretation that in presence of 150 mM NaCl OSEA.HCl undergoes a lamellar gel to liquid crystalline phase transition, whereas in water above phase transition temperature micellar phase is formed. The possibility of the phase transition being due to a micelle order-disorder transition can be discounted based on the very small enthalpy associated with such transitions. For example, sphingosine-1-phosphate micelles undergo an order-disorder transition at 65 °C, with an enthalpy of 0.34 kcal/mol [55].

Spin-label ESR spectroscopy employing fatty acid or phospholipid spin labels bearing stable nitroxide spin probes have been used extensively to study the environment in the hydrophobic region of lipid aggregates and membranes [30,56,57]. The outer hyperfine splitting

($2A_{max}$) of the probe provides information regarding the structure and dynamics of lipid aggregates. The observed $2A_{max}$ values of 5-doxylstearic acid embedded in OSEA.HCl dispersed in water and in 150 mM NaCl at low temperature (below phase transition) are comparable to the $2A_{max}$ values obtained for this spin label in the lamellar gel phase of different lipids [29–31]. The ESR spectrum recorded above transition temperature in aqueous dispersions was more isotropic, which is consistent with a micellar structure. In presence of 150 mM salt the ESR spectrum was relatively more anisotropic even after the phase transition and displays features that are characteristic of a fluid liquid crystalline phase with partially motionally averaged, axial hyperfine anisotropy [29]. The obtained $2A_{max}$ values are in the range of values observed for this spin label in liquid crystalline phase [30,31,33]. The ESR data and the bluish turbidity of the sample suggest the presence of liquid crystalline phase above the phase transition temperature (Figs. 3 and 4).

### *4.1. Effect of salt on the phase behavior of O-stearoylethanolamine hydrochloride*

The influence of ions on the structure and function of biological membranes is well recognized and the effects of ions on natural membranes as well as on model systems have been extensively investigated [15–22]. For a charged lipid in water, due to electrostatic repulsion the effective head group size of charged lipids increases and above the phase transition, for some lipids the lamellar fluid phase will be unstable due to more open head group structure and it will most likely transform to a micellar phase. This type of phase transition has been characterized in surfactants, platelet activating factor and also in important derivatized lipids such as *N*-biotinyl phosphatidylethanolamines [58–64]. Increase in the ionic strength of the aqueous solution of single-tailed ionic surfactants may result in a decrease in the head group area, which increases the value of packing parameter *P* towards one, which stabilizes the bilayer gel and liquid crystalline phases. In the present study it was observed that presence of 150 mM NaCl stabilizes the bilayer structure of OSEA.HCl.

### *4.2. Structure and phase behavior*

Previous biophysical studies suggest that *N*-acylethanolamines and their precursors, i.e., *N*-acylphosphatidylethanolamines stabilize the bilayer structure of phospholipids in which they are incorporated, most likely due to their strong tendency to form bilayer structure [47,65,66]. The crystal structure of NAEs with different fatty acyl chainlengths namely, *N*-stearoylethanolamine, *N*-palmitoylethanolamine and *N*-myristoylethanolamine also revealed that these molecules are packed in a bilayer fashion with tail-to-tail chain packing [37–39]. *O*-acylethanolamines are structural isomers of NAEs and analysis of the crystal structure of *O*-stearoylethanolamine hydrochloride revealed that the acyl chains in this lipid are also packed in a bilayer fashion. Although both NAEs and OSEA.HCl adopt a bilayer structure in the solid state the structure of individual molecules in these two classes of compounds is different. While NAEs adopt an L shape in the solid state, OSEA.HCl adopts a linear shape. The different shapes may result in differences in the type of interaction with other membrane lipids such as phospholipids, lysolipids and cholesterol.

The tilt angle with respect to bilayer normal in OSEA.HCl was found to be 44.4°, which is much higher than the values found in NAEs with different chainlengths [37–39]. The chain tilt is a consequence of large head group and the packing problem is overcome by the tilting of the hydrocarbon chains with respect to the bilayer normal. Other biologically relevant single-chain lipids such as lysophosphatidic acid and lysophosphatidylethanolamine also have large head group areas due to which they pack in a bilayer format with high tilt angle of the acyl chains with respect to the bilayer normal [67,68]. It was observed that if the tilt angle is more than 60° it induces interdigitation in the acyl chain packing [26]. In OSEA.HCl the bulky $Cl^-$ counterions may induce higher chain tilt as compared to NAEs and it is expected that in water, hydration will make the effective head group area even larger. Such increase in head group area may induce tilt in the chains with respect to bilayer plane.

## 5. Conclusions

Biophysical investigations using DSC, turbidimetry, spin-label ESR, fluorescence and low-angle X-ray scattering have been employed in order to characterize the phase behavior of *O*-stearoylethanolamine, a member of new class of lipid called *O*-acylethanolamines. These studies indicate that in the hydrated state OSEA undergoes a phase transition centered at 53.8 °C and ionic strength may modulate the transition temperature and the phase structure above the phase transition. All the results from different biophysical techniques fit well if one assumes that *O*-stearoylethanolamine dispersed in water undergoes a lamellar gel to micellar phase transition, whereas in presence of salt it undergoes a lamellar gel to liquid crystalline phase transition. The first crystal structure of an *O*-acylethanolamine molecule, namely *O*-stearoylethanolamine hydrochloride (OSEA.HCl) has been solved by single-crystal X-ray diffraction. The structure demonstrates that the OSEA.HCl molecules adopt a bilayer-type arrangement with tail-to-tail chain packing. The stabilization of bilayer structure of single-tailed membrane components even at high temperature in presence of physiological salt concentration may be useful to understand the role of ionic strength on the membrane structure under stress, for example, at high temperatures in extremophiles.

## Acknowledgements

This work was supported by a research project from the Department of Science and Technology (India) to MJS. PKT is a Senior Research Fellow of Council of Scientific and Industrial Research (CSIR) (India). We thank Prof. V. A. Raghunathan (Raman Research Institute, Banglore) for the use of the Hecus S3-Micro SAXS apparatus, and Mr. Madhukar and Mr. Santosh for their help in measurements with it. Use of the National Single-Crystal Diffractometer Facility (SMART APEX CCD single-crystal X-ray diffractometer) at the School of Chemistry, University of Hyderabad, funded by Department of Science and Technology (India) is gratefully acknowledged. We thank the University Grants Commission (India) for their support through the UPE (to University of Hyderabad), CAS (to School of Chemistry) programs. The authors are grateful to Prof. Samudranil Pal of this School and Dr. Archan Dey for advice in X-ray data analysis.

## References

[1] D. Stetten Jr., Biological synthesis of choline by rats on diets with and without adequate lipotropic methyl, J. Biol. Chem. 142 (1941) 629–633.
[2] H. Kewitz, O. Pleul, Synthesis of choline from ethanolamine in rat brain, Proc. Natl Acad. Sci. U. S. A. 73 (1976) 2181–2185.
[3] H.H.O. Schmid, P.C. Schmid, V. Natarajan, *N*-Acylated glycerophospholipids and their derivatives, Prog. Lipid Res. 29 (1990) 1–43.
[4] K.D. Chapman, Occurrence, metabolism, and prospective functions of *N*-acylethanolamines in plants, Prog. Lipid Res. 43 (2004) 302–327.
[5] W.A. Devane, L. Hanus, A. Breuer, R.G. Pertwee, L.A. Stevensen, G. Griffin, D. Gibson, A. Mandelbaum, A. Etinger, R. Mechoulam, Isolation and structure of a brain constituent that binds to the cannabinoid receptor, Science 258 (1992) 1946–1949.
[6] H. Scheul, E. Goldstein, R. Mechoulam, A.M. Zimmerman, S. Zimmerman, Anandamide (arachidonylethanolamide), a brain cannabinoid receptor agonist, reduces sperm fertilizing capacity in sea urchins by inhibiting the acrosome reaction, Proc. Natl Acad. Sci. U. S. A. 91 (1994) 7678–7682.
[7] L. Venance, D. Piomelli, J. Glowinski, C. Giaume, Inhibition of anandamide of gap junctions and intercellular calcium signaling in striatal astrocytes, Nature 376 (1995) 590–594.
[8] L. Facci, R. Dal Toso, S. Romanello, A. Buriani, S.D. Skaper, A. Leon, Mast cells express a peripheral cannabinoid receptor with differential sensitivity to anandamide and palmitoylethanolamide, Proc. Natl Acad. Sci. U. S. A. 92 (1995) 3376–3380.

[9] K.D. Chapman, S. Tripathy, B. Venables, A.D. Desouja, *N*-Acylethanolamines: formation and molecular composition of a new class of plant lipids, Plant Physiol. 116 (1998) 1163–1168.
[10] S.P. Markey, T. Dudding, T.L. Wang, Base- and acid-catalyzed interconversions of *O*-acyl and *N*-acyl-ethanolamines: a cautionary note for lipid analyses, J. Lipid Res. 41 (2000) 657–662.
[11] R.F. Murphy, S. Powers, C.R. Cantor, Endosome pH measured in single cells by dual fluorescence flow cytometry: rapid acidification of insulin to pH 6, J. Cell Biol. 98 (1984) 1757–1762.
[12] S.L. Rybak, R.F. Murphy, Primary cell cultures from murine kidney and heart differ in endosomal pH, J. Cell. Physiol. 176 (1998) 216–222.
[13] J.A. Boomer, D.H. Thompson, Synthesis of acid-labile diplasmenyl lipids for drug and gene delivery applications, Chem. Phys. Lipids 99 (1999) 145–153.
[14] A.C. Porter, J-M. Sauer, M.D. Knierman, G.W. Becker, M.J. Berna, J. Bao, G.G. Nomikos, P. Carter, F.P. Bymaster, A.B. Leese, C.C. Felder, Characterization of a novel endocannabinoid, virodhamine, with antagonist activity at the CB1 receptor, J. Pharmacol. Exp. Ther. 301 (2002) 1020–1024.
[15] A. Aroti, E. Leontidis, M. Dubois, T. Zemb, Effects of monovalent anions of the hofmeister series on DPPC lipid bilayers Part I: swelling and in-plane equations of state, Biophys. J. 93 (2007) 1580–1590.
[16] R.A. Böckmann, A. Hac, T. Heimburg, H. Grubmüller, Effect of sodium chloride on a lipid bilayer, Biophys. J. 85 (2003) 1647–1655.
[17] S. Garcia-Manyes, G. Oncins, F. Sanz, Effect of ion-binding and chemical phospholipid structure on the nanomechanics of lipid bilayers studied by force spectroscopy, Biophys. J. 89 (2005) 1812–1826.
[18] P.M. Macdonald, J. Seelig, Anion binding to neutral and positively charged lipid membranes, Biochemistry 27 (1988) 6769–6775.
[19] G. Pabst, A. Hodzic, J. Strancar, S. Danner, M. Rappolt, P. Laggner, Rigidification of neutral lipid bilayers in the presence of salts, Biophys. J. 93 (2007) 2688–2696.
[20] H.I. Petrache, S. Tristram-Nagle, D. Harries, N. Kucerka, J.F. Nagle, V.A. Parsegian, Swelling of phospholipids by monovalent salt, J. Lipid Res. 47 (2006) 302–309.
[21] P. Sapia, L. Coppola, G. Ranieri, L. Sportelli, Effects of high electrolyte concentration on DPPC-multilayers: an ESR and DSC investigation, Colloid Polym. Sci. 272 (1994) 1289–1294.
[22] H. Träuble, H. Eibl, Electrostatic effects on lipid phase transitions: membrane structure and ionic environment, Proc. Natl Acad. Sci. U. S. A. 71 (1974) 214–219.
[23] R. Glaser, Echinocyte formation induced by potential changes of human red blood cells, J. Membr. Biol. 66 (1982) 79–85.
[24] A. Herrmann, P. Müller, Ionic strength-dependent alterations of membrane structure of red blood cells, Biosci. Rep. 6 (1986) 1007–1015.
[25] G.M. Sheldrick, SHELXL97 Program for the refinement of crystal structures, University of Göttingen, Göttingen, Germany, 1997.
[26] P.L. Yeagle, The structure of biological membranes, 2nd edition. CRC press, 2005.
[27] R.N.A.H. Lewis, N. Mak, R.N. McElhaney, A differential scanning calorimetric study of the thermotropic phase behavior of model membranes composed of phosphatidylcholines containing linear saturated fatty acyl chains, Biochemistry 26 (1987) 6118–6126.
[28] J.H. Kleinschmidt, D. Marsh, Spin-label electron spin resonance studies on the interactions of lysine peptides with phospholipid membranes, Biophys. J. 73 (1997) 2546–2555.
[29] M.B. Sankaram, T.E. Thompson, Interaction of cholesterol with various glycerophospholipids and sphingomyelin, Biochemistry 29 (1990) 10670–10675.
[30] Y.V.S. Rama Krishna, D. Marsh, Spin label ESR and $^{31}$P-NMR studies of the cubic and inverted hexagonal phases of dimyristoylphosphatidylcholine/myristic acid (1:2, mol/mol) mixtures, Biochim. Biophys. Acta 1024 (1990) 89–94.
[31] D. Marsh, Molecular motion in phospholipids bilayers in the gel phaae: long axis rotation, Biochemistry 19 (1980) 1632–1637.
[32] C.R. Benatti, E. Feitosa, R.M. Fernandez, M.T. Lamy-Freund, Structural and thermal characterization of dioctadecyldimethylammonium bromide dispersions by spin labels, Chem. Phys. Lipids 111 (2001) 93–104.
[33] J. Pérez-Gil, C. Casals, D. Marsh, Interactions of hydrophobic lung surfactant proteins SP-B and SP-C with dipalmitoylphosphatidylcholine and dipalmitoylphosphatidylglycerol bilayers studied by electron spin resonance spectroscopy, Biochemistry 34 (1995) 3964–3971.
[34] K. Kalyanasundaram, J.K. Thomas, Environmental effects on vibronic band intensities in pyrene monomer fluorescence and their application in studies of micellar systems, J. Am. Chem. Soc. 99 (1977) 2039–2044.
[35] S. Georghiou, A.K. Mukhyopadhyay, Phase transitions and cholesterol effects in phospholipid liposomes. A new method employing the enhancement of the O–O vibronic transition of pyrene, Biochim. Biophys. Acta 645 (1981) 365–368.
[36] I. Pascher, M. Lundmark, P.G. Nyholm, S. Sundell, Crystal structures of membrane lipids, Biochim. Biophys. Acta 1113 (1992) 339–373.
[37] B. Dahlén, I. Pascher, S. Sundell, The crystal structure of *N*-(2-hydroxyethyl)-octadecanoate, Acta. Chim. Scand. A. 31 (1977) 313–320.
[38] M. Ramakrishnan, M.J. Swamy, Molecular packing and intermolecular interactions in *N*-acylethanolamines: crystal structure of *N*-myristoylethanolamine, Biochim. Biophys. Acta 1418 (1999) 261–267.
[39] R.K. Kamlekar, M.J. Swamy, Molecular packing and intermolecular interactioms in two structural polymorphs of *N*-palmitoylethanolamine, a type-2 cannabinoid receptor agonist, J. Lipid Res. 47 (2006) 1424–1433.
[40] S. Abrahamsson, B. Dahlén, H. Löfgren, I. Pascher, Lateral packing of hydrocarbon chains, Prog. Chem. Fats Lipids 16 (1978) 125–143.
[41] P.R. Maulik, M.J. Ruocco, G.G. Shipley, Hydrocarbon chain packing modes in lipids: effect of altered sub-cell dimensions and chain rotation, Chem. Phys. Lipids 56 (1990) 123–133.
[42] O. Ermer, A. Eling, A, Molecular recognition among alcohols and amines: super-tetrahedral crystal architectures of linear diphenol–diamine complexes and aminophenols, J. Chem. Soc., Perkin Trans. 2 (1994) 925–944.
[43] M.J. Swamy, M. Ramakrishnan, D. Marsh, Miscibility and phase behaviour of binary mixtures of *N*-palmitoylethanolamine and dipalmitoylphosphatidylcholine, Biochim. Biophys. Acta 1616 (2003) 174–183.
[44] I. Yamashita, Y. Kawabata, T. Kato, M. Hato, H. Minamikawa, Small angle X-ray scattering from lamellar phase for β-3, 7-dimethyloctylglucoside/water system: comparison with β-n-alkylglucosides, Colloids Surf., A Physicochem. Eng. Asp. 250 (2004) 485–490.
[45] V.K. Aswal, P.S. Goyal, S. De, S. Bhattacharya, H. Amenitsch, S. Bernstorff, Small-angle X-ray scattering from micellar solutions of gemini surfactants, Chem. Phys. Lett. 329 (2000) 336–340.
[46] P.E. Harper, D.A. Mannock, R.N.A.H. Lewis, R.N. McElhaney, S.M. Gruner, X-ray diffraction structures of some phosphatidylethanolamine lamellar and inverted hexagonal phases, Biophys. J. 81 (2001) 2693–2706.
[47] A. Ambrosoni, E. Bertoli, P. Mariani, E. Tanfani, M. Wozniak, G. Zolese, *N*-Acylethanolamines as membrane topological stress compromising agents, Biochim. Biophys. Acta 1148 (1993) 351–355.
[48] R.K. Kamlekar, S. Satyanarayana, D. Marsh, M.J. Swamy, Miscibility and phase behavior of *N*-acylethanolamine/diacylphosphatidylethanolamine binary mixtures of matched acyl chainlengths ($N=14, 16$), Biophys. J. 92 (2007) 3968–3977.
[49] R.K. Kamlekar, M.S. Chandra, T.P. Radhakrishnan, M.J. Swamy, Interaction of *N*-myristoylethanolamine with cholesterol investigated in a Langmuir film at the air–water interface, Biophys. Chem. 139 (2009) 63–69.
[50] D. Marsh, M.J. Swamy, Derivatized lipids in membranes: physico-chemical aspects of *N*-biotinyl phosphatidylethanolamines, *N*-acyl phosphatidylethanolamines and *N*-acylethanolamines, Chem. Phys. Lipids 105 (2000) 43–69.
[51] M. Ramakrishnan, V. Sheeba, S.S. Komath, M.J. Swamy, Differential scanning calorimetric studies on the thermotropic phase transitions of dry and hydrated forms of *N*-acylethanolamines of even chainlengths, Biochim. Biophys. Acta 1329 (1997) 302–310.
[52] M. Ramakrishnan, R. Kenoth, K. Ravikanth, M.S. Chandra, T.P. Radhakrishnan, M.J. Swamy, *N*-Myristoylethanolamine – cholesterol (1:1) complex: first evidence from differential scanning calorimetry, fast-atom-bombardment mass spectrometry and computational modeling, FEBS Lett. 531 (2002) 343–347.
[53] M.J. Swamy, M. Ramakrishnan, D. Marsh, U. Würz, Miscibility and phase behaviour of binary mixtures of *N*-palmitoylethanolamine and dipalmitoylphosphatidylcholine, Biochim. Biophys. Acta 1616 (2003) 174–183.
[54] J.N. Israelachvili, Intermolecular and Surface Forces, Academic Press, New York, 1992.
[55] M. García-Pacios, M.I. Collado, J.V. Busto, J. Sot, A. Alonso, J.L. Arrondo, F.M. Goni, Sphingosine-1-phosphate as an amphipathic metabolite: its properties in aqueous and membrane environments, Biophys. J. 97 (2009) 1398–1407.
[56] M.J. Swamy, D. Marsh, Spin-label electron spin resonance studies on the dynamics of the different phases of *N*-biotinylphosphatidylethanolamines, Biochemistry 33 (1994) 11656–11663.
[57] M.J. Swamy, M. Ramakrishnan, B. Angerstein, D. Marsh, Spin-label electron spin resonance studies on the mode of anchoring and vertical location of the *N*-acyl chain in *N*-acylphosphatidylethanolamines, Biochemistry 39 (2000) 12476–12484.
[58] A. Ohta, S. Nakashima, H. Matsuyanagi, T. Asakawa, S. Miyagishi, Krafft temperature and enthalpy of solution of *N*-acyl amino acid surfactants and their racemic modifications: effect of the counter ion, Colloid Polym. Sci. 282 (2003) 162–169.
[59] F.R. Alves, M.E.D. Zaniquelli, W. Loh, E.M.S. Castanheira, M.E.C.D. Real Oliveira, E. Feitosa, Vesicle-micelle transition in aqueous mixtures of the cationic dioctadecyldimethylammonium and octadecyltrimethylammonium bromide surfactants, J. Colloid Interface Sci. 316 (2007) 132–139.
[60] E. Feitosa, N.M. Bonassi, W. Loh, Vesicle-micelle transition in mixtures of dioctadecyldimethylammonium chloride and bromide with nonionic and zwitterionic surfactants, Langmuir 22 (2006) 4512–4517.
[61] K. Horbaschek, H. Hoffmann, C. Thunig, Formation and properties of lamellar phases in systems of cationic surfactants and hydroxy-naphthoate, J. Colloid Interface Sci. 206 (1998) 439–456.
[62] C. Huang, J.T. Mason, F.A. Stephenson, I.W. Levin, Polymorphic phase behavior of platelet-activating factor, Biophys. J. 49 (1986) 587–595.
[63] N. Maurer, P. Elmar, P. Fritz, G. Otto, Phase behavior of the antineoplastic ether lipid 1-*O*-octadecyl-2-*O*-methylglycero-3-phosphocholine, Biochim. Biophys. Acta 1192 (1994) 167–176.
[64] M.J. Swamy, U. Würz, D. Marsh, Structure of vitaminylated lipids in aqueous dispersion: X-ray diffraction and $^{31}$P NMR studies of *N*-biotinylphosphatidylethanolamines, Biochemistry 32 (1993) 9960–9967.
[65] J. Domingo, M. Mora, M.A. De Madariaga, Incorporation of *N*-acylethanolamine phospholipids into egg phosphatidylcholine vesicles: characterization and permeability properties of the binary systems, Biochim. Biophys. Acta 1148 (1993) 308–316.
[66] M. Mercadal, J.C. Domingo, M. Bermudez, M. Mora, M.A. De Madariaga, *N*-Palmitoylphosphatidylethanolamine stabilizes liposomes in the presence of human serum: effect of lipidic composition and system characterization, Biochim. Biophys. Acta 1235 (1995) 281–288.
[67] I. Pascher, S. Sundell, H. Hauser, Polar group interaction and molecular packing of membrane lipids. The crystal structure of lysophosphatidylethanolamine, J. Mol. Biol. 153 (1981) 807–824.
[68] I. Pascher, S. Sundell, Interactions and space requirements of the phosphate head group in membrane lipids. The crystal structure of disodium lysophosphatidate dehydrate, Chem. Phys. Lipids 37 (1985) 241–250.